CRACK GROWTH IN PRESSURE VESSELS UNDER CREEP CONDITIONS

M. C. Coleman, A. T. Price and J. A. Williams*

INTRODUCTION

The occurrence of crack like defects in welded components in CEGB plant operating in the creep range has required the development of techniques for analysing crack growth in these structures. The methods developed have been extensions from conventional fracture mechanics as applied in fatigue and brittle fracture analyses. Crack growth data have been obtained for a wide variety of creep resistant materials using conventional, relatively small, uniaxial specimens and various correlations have been proposed relating crack growth rate to parameters such as stress intensity factor (K), reference stress (σ_{ref}), crack opening displacement (COD) and displacement rate ($\dot{\delta}$). Clearly, it is necessary to examine the validity of such correlations in real large scale structures to establish creep crack growth mechanics with respect to the more established areas of fracture mechanics and against the background of engineering methods used for design against creep. This paper deals with the first experiment in a programme on large pressure vessels designed to examine the extent to which current ideas developed from small scale laboratory tests can be applied to components used in power generating plant. It describes the design of and creep deformation and crack growth in a vessel fabricated from 1/2CrMoV pipe tested under steam pressure containment conditions.

EXPERIMENTAL

The main objective of this, the first pressure vessel experiment, was to induce failure by crack growth, to assess the applicability of existing crack growth descriptions, and to allow subsequent experiments to be defined more precisely. A simple pipe geometry containing circumferential machined notches was selected because in plant a large proportion of failures occur in this plane as a result of heat affected zone cracking. The material was normalised and tempered 1/2CrMoV steel.

Shell Design

This geometry requires careful design of the shell as the hoop stress will be greater than the axial stress driving the crack and could lead to failure by an axial split. The hoop creep deformation is determined by the equivalent stress produced in the shell. Various forms of equivalent stresses can be calculated and depend on the yield criteria and the stress position. For thin wall cylinders:

$$\sigma_{mdh} = PD_m/2W \qquad (1)$$

*Central Electricity Generating Board, Marchwood Engineering Laboratories, Marchwood, Southampton, England.

where P is the internal pressure, W the wall thickness, σ_{mdh} the mean diameter hoop stress and D_m, the mean diameter.

For thick wall cylinders, Soderberg [1] modified this to:

$$\sigma = \sqrt{3}\, PD_m/4W \qquad (2)$$

Alternatively, the reference stress approach [2,3,4] can be used, where σ_{ref} is the stress which when applied to a uniaxial specimen gives the same displacement rate. For a thick wall cylinder:

$$\sigma_{ref} = \{QP/(R^2-1)\}\ \{(R^2-1)/n(R^{2/n}-1)\}^{n/n-1} \qquad (3)$$

where Q is 2 for the Tresca and $\sqrt{3}$ for the von Mises criterion, R is the pipe diameter ratio and n is the creep rate:stress index. σ_{ref} is virtually independent of n and for the Tresca criterion gives the same stress as equation (1) and for the von Mises criterion gives the same stress as equation (2).

From an examination of mean life, ISO creep rutpure data (5) at 838K the steam pressure was set at 62.5 MPa, for which the corresponding shell hoop and axial stresses and lives are given in Table 1.

Notch Design

When this work was initiated only limited data were available* on creep crack growth in normalised and tempered 1/2CrMoV steel. Two relationships were postulated:

$$da/dt = CK^b \qquad (4)$$

where the bounds gave $C=10^{-13}$ and 10^{-14} with b=6 in units of m/hr and MPa.$m^{1/2}$ and, alternatively:

$$da/dt = D\sigma_{net}^c \qquad (5)$$

where the bounds were $D = 5.8 \times 10^{-23}$ and 1.1×10^{-23} with c = 7.4 and the net section stress, σ_{net}, in MPa.

The formula for a full circumferential crack in a hollow cylinder [7] was used to calculate the stress intensity factor:

$$K = \sigma_{gross}\, a^{1/2}\, f(a/W) \qquad (6)$$

and equations (4) and (6) were integrated numerically to obtain curves of crack length (a) as a function of time. Similar curves were generated from equation (5) where σ_{net} was the axial load due to pressure acting over the ligament area defined by (W-a). These computations led to the vessel design shown in Figure 1; the notches were 30mm, 28mm, 27mm and 24mm in depth, and life predictions for the various failure modes are given in Table 1. These conditions were intended to produce failure by crack growth from the

*This data was made available by Neate who subsequently concluded [6] from the results of further work that crack growth rate was best described by correlation with σ_{ref}.

30mm notch; the depths of the other notches being selected to produce lesser amounts of crack growth based on the notional relationship given in equation (4). Note that σ_{net} in equation (5) is equal to σ_{ref}. As can be seen in Figure 1 the vessel also contained two part circumferential defects, but these will not be discussed rurther in this paper.

Vessel Fabrication and Monitoring

The bore and outside diameter of the pipe were machined and the notches cut as the final operation before welding on the end caps; details are given in Figure 1. The notch spacings were determined by elasticity calculations (8) which showed that there is negligible interaction at a spacing of five times the crack depth. The spacing of the defects from the end caps calculated by an elastic reep analysis (9) allowed a maximum of 10% increase in stress at the position where the elastic stress concentration from the defect above was negligible.

The vessel was tested in a purpose built Pressure Vessel Testing Facility using internal steam pressure at 62.5 MPa and positioned vertically within a bell furnace in which the temperature was maintained at 838K ± 5K. During the test, crack growth was monitored continuously using the potential drop technique at four positions at 90° intervals around the circumference of the 30mm deep notch. Acoustic emission monitoring was also employed to detect activity in the vessel in general and, using a coincidence counting technique, at the 30mm notch in particular. In addition, capacitance strain gauges were used to monitor displacement across the 28mm deep notch. Intermittent inspections were also carried out at ambient temperature and, on these occasions, creep strain occurring in the shell was measured across bosses welded at mid positions between defects and displacements across the notches were measured using slip gauges. A more detailed description of the facility and associated measuring methods can be found elsewhere [10,11].

RESULTS

At the first inspection of 290 hours no crack growth was found on any notch. Subsequently at approximately 700 hours acoustic output was detected on the 30mm notch and the potential drop records indicated that crack growth had also commenced. This was confirmed by an inspection at 1192 hours, when cracking was evident on all defects. The ultrasonic examination showed, however, that crack growth was occurring asymmetrically on the 30mm notch and this was accompanied by an increase in edge opening displacement (EOD) and creep displacement across this defect; this was manifest on the vessel as an apparent bending, albeit small. Further inspections were carried out at 1361 and 1577 hours and, at 1583 hours, the vessel failed explosively across the reduced ligament section of the original 30mm notch.

Examination of the fracture surface confirmed the asymmetry of the crack front for the largest notch; final failure having been induced by a change in failure mechanism from creep crack growth to fast shear failure. Details of this examination will be reported elsewhere.

Selected results, illustrating the general deformation of the vessel are shown in Table 2, which contains data relating to creep strains measured diametrically at the mid-points between the defects and axially across these mid-points. Within the limits of experimental accuracy, the creep rates remained steady throughout the test. The cross sections adjacent to the 24mm and 27mm notches remained circular, although there was some

indication of ellipticity adjacent to the 28mm notch and clear evidence adjacent to the 30mm notch. The effects were not large, the minimum and maximum diametral strains being 0.72% and 0.84% respectively just before failure; the latter value being obrained across the diameter traversing maximum and minimum crack growth. The creep deformations measured axially across the mid notch positions for all but the deepest notch agreed reasonably well with the diametral strains indicating an approximate 1:1 relationship between hoop and axial deformation. This correlation is thought to be fortuitous as examination of the edge opening displacements (see below) indicates greater axial strains than derived from the micrometer measurements given in Table 2. From this and other detailed examinations, it was concluded that the change of shape arose from general creep deformation accompanied by *bulging* at the two largest notches; this was the cause of the apparent bending of the vessel.

While the general temperature control during the experiment was ± 5K detailed examination of the records showed that the temperature of the vessel decreased by 5K from the top (A) to the bottom (D). If allowance is made for this difference, then the hoop creep strains measured on the vessel are in good agreement at all positions except adjacent to the 30mm notch where the bulging effect caused a more rapid creep rate on the side where crack growth was largest.

The results obtained across the 30mm notch using the ptoential drop technique are shown in Figure 2 and illustrate the asymmetry of crack growth. Other data on crack length measurements are shown in Table 3. The values determined ultrasonically were accurate to ± 2mm and, while this is good in practical terms, it does not allow crack growth rate at low rates to be established very precisely. The crack lengths obtained after failure by sectioning techniques agree well with those determined by the other methods and confirm the differences in crack growth on the opposite side of the 30mm notch. However, they also show that the 24mm and 27mm notches grew uniformly around the circumference.

Data on EOD are given in Table 4. It can be seen that the EOD across the 30mm defect was a factor of 3 larger on the side experiencing the faster crack growth rate. The data also indicate an increasing EOD rate with time, although the data on the smaller defects could easily be regarded as constant with time. Similar comments apply to the measurements of crack length where the potential measurements across the 30mm notch show an increasing crack growth rate, whereas the data for the other notches are less precise and do not allow firm conclusions to be drawn.

DISCUSSION

The acoustic emission and potential drop evidence indicate that crack initiation for the 30mm notch occurred at ~ 700 hours, and all notches were seen to have initiated cracks by 1192 hours. The exact time for crack initiation at the 24mm and 27mm notches is not known and there is considerable scope for interpretation within the timescale of the 290-1192 hours interval between inspections. Nevertheless, although these is typically a factor of about two difference in EOD around each defect, the EOD data are generally self consistent and suggest that the EOD to initiate cracking increases with notch depth. Also comparison with Table 1 indicates that larger displacements are needed to produce incremental crack growth on the cracks growing from larger initial notches. These observations suggest that the crack initiation and growth mechanisms can

probably be interpreted in terms of a constant $\dot{\delta}.t$ product analogous to the constant $\dot{\varepsilon}.t$ product commonly used to describe creep failure.

One method of describing the crack growth data is to put:

$$\dot{a} = \dot{\delta}^m \qquad (7)$$

Haigh [12] related $\dot{\delta}$, taken as the COD rate, to the equivalent stress, σ_E, calculated from time independent elastic-plastic analysis; where σ_E is σ_{gross} multiplied by the yield stress ratio of the uncracked and cracked geometries. Actually it transpires [13] that the plane stress value of σ_E is the same as σ_{ref}, the effective creep stress. In the present instance, the difficulty is to relate the EOD measured using slip gauges to COD. Notionally, it might be expected that the EOD in the vessel experiment would be identical to the axial strain occurring across the ligament. However, the bulging effect produced a rotation across each notch. The amount was small; for example, the total included angle varied from 0.5° to 2.5° around the 28mm notch. Thus the EOD is larger than the real COD and a correction factor is necessary if a comparison is to be made with the laboratory data. It can be shown that the angles measured are consistent with those which would be obtained at displacements up to 2mm if the defects were loaded as in compact tension or single edge notched specimens. For the defect geometries used here the δ/EOD ratio is approximately 0.3. Applying this factor and calculating crack growth rates as averages between successive inspection periods, or directly from Figure 2, $\dot{a}$ has been plotted in Figure 3 as a function of $\dot{\delta}$ determined, again by averaging. The bars shown refer to the maximum and minimum $\dot{a}$; the error of the EOD measurements is ~ ± 0.5mm corresponding to about ± 2% error on displacement rate for the 30mm notch. Bounds have been drawn for a 1:1 correlation, Haigh [12] found m = 0.69 and his data fall within the scatter band. Little positive comment is possible with such data and the exact form of the relationship, if any, between $\dot{a}$ and $\dot{\delta}$ is unclear. If account is taken of the crack initiation data, it could be inferred that any correlation is fortuitous. A practical point is that small, 250μm, CODs can initiate cracking and the displacement rates are correspondingly low, even in this relatively ductile 1/2CrMoV. Also intermediate calculations relating $\dot{\delta}$, σ and $\dot{a}$ to material behaviour are needed to apply the data to components and effects such as bulging have to be anticipated. The latter would appear to exclude the use of crack opening angle [14] as a general method of predicting crack growth, although the existing methods used for single edge notch and compact tension geometries should bound the changes resulting from bulging.

The main source of crack growth data is the continuous potential drop records obtained from the 30mm notch which has been analysed in terms of the notional K value and σ_{net}. The latter is σ_{ref} for a pipe loaded axially in tension and, although $\dot{a}$ varied by a factor of ~ 1.5 around the circumference, the actual crack length did not differ by > ~ 10% so that K and σ_{net} are reasonably precise. The equations are:

$$\dot{a} = 10^{-30} K^{18.5} \qquad (8)$$

and

$$\dot{a} = 10^{-38} \sigma_{net}^{16} \qquad (9)$$

The results obtained from ultrasonic and post failure inspections of the 30mm and the smaller initial notches were also analysed separately and were found to be consistent with these equations. Assuming crack initiation from the 30mm notch at 700 hours the lives predicted by equations (8) and

(9) are 735 hours and 1317 hours respectively.

Comparing these equations with Neate's data [6] obtained on small specimens of similar composition, Figures 4 and 5, and with the original design predictions, Table 1, the initial conclusion is that $\dot{a}$ is consistent with a K correlation. However, this direct comparison does not allow for the bulging that took place in the vessel which, by analogy with fracture analysis at ambient temperature, will modify the stress field.

For elastic deformation in an internally pressurised cylinder containing a through thickness circumferential crack Folias [15] has shown that the stress term may be scaled by the factor:

$$m = (1 + 0.165\ c^2/Rt)^{1/2} \qquad (10)$$

where 2c is the crack length.

This will obviously be an overestimate for a part through thickness defect but is used here in the absence of an alternative. Taking c as πR_m gives a scaling factor of 2.2 to be applied directly to the value of K calculated from the Harris formula [7]. The effect of this operation is shown in Figure 4. The new relationship is:

$$\dot{a} = 7 \times 10^{-33}\ K_F^{16} \qquad (11)$$

The effect of bulging on σ_{ref} can be estimated using a modification of the Folias analysis following Hahn and Rosenfield [16] and Keifner et al [17], where the stress factor, S_c is:

$$S_c = (W - a/m)/(W-a) \qquad (12)$$

This was derived experimentally from conventional, below the creep range, fracture mechanics analyses of cylindrical pressure vessels, containing part through axial defects, pressurised to failure. This factor should be valid for the creep of material of high creep rate:stress index, whose behaviour is expected to be similar to that of an elastic plastic material [13]. This is supported by results obtained by Guest and Hutchings [18] obtained from the analysis of creep failures in thin wall tubes containing part through axial defects although direct evidence of its applicability to part through circumferential defects is limited to a few experiments on thin wall tubes pressurised to failure at ambient temperature [19]. For a full circumferential defect of c = 0.55m, S has the values 1.41, 1.61, 1.92 and 2.43 when a/W is 0.4, 0.5, 0.6 and 0.7 respectively.

Recalculation of σ_{ref} on this basis gives the relationship:

$$\dot{a} = 10^{-26}\ \sigma_{ref}^{9} \qquad (13)$$

which is shown in Figure 5.

Applying S_c, without justification, to modify the notional K values gives:

$$\dot{a} = 10^{-19} K_{mod}^{8.5} \qquad (14)$$

which has also been drawn on Figure 4.

The general effect of the bulging corrections is to associate particular $\dot{a}$ values with high K and σ_{ref}, at the same time reducing the indices to values nearer those obtained in the laboratory work. This also leads to a different conclusion regarding the parameter that best describes crack growth in the vessel. Considering the uncorrected data there is good agreement with K but the crack growth rates predicted by σ_{ref} are very much lower. In contrast, the corrected σ_{ref} relationship is quite consistent with the laboratory data obtained [6] on a wide range of geometries and indicates a time of 1579 hours for crack growth for the 30mm notch, which is acceptable. Hence the agreement of $\dot{a}$ with K and the consequent good original prediction of vessel life seems to be fortuitous, reflecting the particular crack geometry and steam pressure conditions chosen to produce failure in a relatively short testing period. However, as a cautionary note, there must be reservations on the above conclusion because neither of the correction factors, for K or for σ_{ref}, has been sufficiently well validated, particularly for the creep regime. Thus, for example, the possiblity of a genuine size effect in a relationship between $\dot{a}$ and K cannot be excluded, although this is considered unlikely in view of the laboratory data. For the present, therefore, a description of crack growth rate in terms of σ_{ref} modified to allow for the effects of bulging appears to be a physically acceptable description for this material, if reservations regarding the correction factor for σ_{ref} are neglected.

As the laboratory data were obtained on specimens up to 50mm thickness and the vessel has a very large, although undefinable, thickness the above conclusion suggests that there is no important size effect in creep crack growth for normalised and tempered 1/2CrMoV at 838K. A vessel test involving somewhat different notch geometries where bulging corrections are lower would allow this uncertainty to be resolved.

CONCLUSION

The interpretation of the relationship between crack growth data and parameters describing stress and geometry is critically dependent on the validity of the correction factor used to allow for the effects of bulging. With this reservation, it is concluded that creep crack growth in this normalised and tempered 1/2CrMoV steel pressure vessel is best described by the reference stress approach.

ACKNOWLEDGEMENT

This paper is published by permission of the Director, Marchwood Engineering Laboratories, Central Electricity Generating Board.

REFERENCES

1. SODERBERG, C. R., Trans. ASME., 63, 1941, 737.
2. ANDERSON, R. G., GARDNER, L. R. T. and HODGKINS, W. R., J. Mech. Engng. Sci., 5, 1963, 238.
3. MACKENZIE, A. C., Int. J. Mech. Sci., 10, 1968, 441.
4. MARRIOT, D. L., Conf. on Creep in Structures, Int. Union Theor. App. Mech, Gothenburg, 1970, Springer-Verlag.
5. HICKIN, W. D., PLASTOW, B. and DAVISON, J. K., SSD MID/M.3/72, 1972.
6. NEATE, G. J. and SIVERNS, M. J., Instn. Mech. Engrs. Int. Conf., Creep and Fatigue in Elevated Temperature Applications, Philadelphia, September 1973 and Sheffield, April 1974.

7. HARRIS, D. O., J. Basic Engng., March 1967, 49.
8. DURELLI, A. J., LAKE, R. L. and PHILLIPS, E. A., Machine Design, December 1951, 165.
9. WALTERS, D. J., CEGB Berkeley Nuclear Laboratories. Private Communication, 1973.
10. EATON, N. F. and ROWLEY, T., Int. Inst. of Welding, Annual Assembly, Toronto Colloquium, 1972.
11. COLEMAN, M. C., FIDLER, R. and WILLIAMS, J. A., Welding Institute Publication, The Detection and Measurement of Cracks, 1976.
12. HAIGH, J. R., Ph.D. Thesis, CNAA London, 1973.
13. WILLIAMS, J. A. and PRICE, A. T., J. Eng. Mats. and Tech., July 1975, 214.
14. FORMBY, C. L., CEGB Report R/B/R2067, 1972.
15. FOLIAS, E. S., Third International Conference on Structural Mechanics in Reactor Technology, 1, Paper C4/5, 1976.
16. HAHN, G. T. and ROSENFIELD, A. R., Acta Met., 13, 1965, 293.
17. KIEFNER, J. F., MAXEY, W. A., EIBER, R. J. and DUFFY, A. R., ASTM STP537, 1973, 461.
18. GUEST, J. C. and HUTCHINGS, J. A., Instn. Mech. Engrs., Int. Conf. Creep and Fatigue in Elevated Temperature Applications, Philadelphia, September 1973 and Sheffield, April 1974.
19. DARLASTON, B. J. L., CEGB Berkeley Nuclear Laboratories, Private Communication, 1976.

Table 1 The pressure vessel shell hoop and axial stresses and corresponding lives for an internal pressure of 62.5 MPa.

Hoop			Axial			
					Life	
Equation	Stress MPa	Life Hours	Stress Position	Stress MPa	Basis	Hours
Thin shell	150	3,500	Gross Section	47.5	ISO	20,000
Thick shell (Soderberg)	130	8,000	Net section at 30mm deep notch	106	CK^6 $C=10^{-13}$	581
Reference stress (Von Mises)	130	8,000	"	"	CK^6 $C=10^{-14}$	5,815
Reference stress (Tresca)	150	3,500				

Table 2 Selected strains indicating the range of hoop and axial deformations measured on the pressure vessel.

Diametral Position	Maximum Diametral Strain (%) after				
	290h	1192h	1361h	1577h	1583h
Above 24mm deep notch	0.09	0.23	0.27	0.31	0.31
Between 24 & 28mm deep notches	0.09	0.32	0.39	0.48	0.48
Between 28 & 30mm deep notches	0.09	0.42	0.56	0.84	0.89
Between 30 & 27mm deep notches	0.08	0.42	0.58	0.84	0.87
Below 27mm deep notch	0.05	0.24	0.30	0.37	0.38

Axial Position		Axial Strain (%) after				
		290h	1192h	1361h	1577h	1583h*
Across 24mm notch.	Max	0.10	0.29	0.34	0.40	-
	Min	0.07	0.15	0.17	0.18	0.04
Across 27mm notch.	Max	0.12	0.45	0.56	0.55	0.55
	Min	0.03	0.14	0.18	0.15	0.16
Across 28mm notch.	Max	0.07	0.47	0.62	0.69	-
	Min	0.05	0.12	0.14	0.08	0.02
Across 30mm notch.	Max	0.10	1.02	1.70	5.11	-
	Min	0.06	0.35	0.50	0.51	-

* Failure of the vessel occurred at this time and the axial strains are subject to doubt because of vessel impact against the containment structure.

Table 3 The average notch depths measured ultrasonically during inspection periods in the test compared with final measurements obtained directly from metallographic sections.

Original Notch depth mm		Ultrasonically measured average depth, mm, after					Final directly measured depth, mm
		290h	1192h	1361h	1577h	1583h	
24	max	24.0	25.0	27.5	26.2	27.2	25.7
	min	24.0	24.0	24.0	24.0	25.5	25.8
27	max	27.0	29.0	31.5	30.7	31.0	30.3
	min	27.0	28.0	30.2	29.7	31.0	30.7
28	max	28.0	31.0	31.2	32.2	31.0	31.3
	min	28.0	29.0	30.2	31.0	30.5	30.5
30	max	30.0	33.7	35.7	38.0	-	-
	min	30.8	32.7	34.5	35.0	-	-

Table 4 Edge opening displacement measured using slip gauges during inspection periods in the test. Original notch widths 3mm.

Original Notch depth mm		Edge opening displacements, mm, after			
		290h	1192h	1361h	1577h
24	max	0.203	0.559	0.686	0.813
	min	0.178	0.330	0.381	0.457
27	max	0.102	0.864	1.118	1.372
	min	0.076	0.330	0.406	0.457
28	max	0.304	1.219	1.549	2.108
	min	0.127	0.533	0.584	0.736
30	max	0.330	2.311	3.759	9.779
	min	0.228	1.219	1.651	2.921

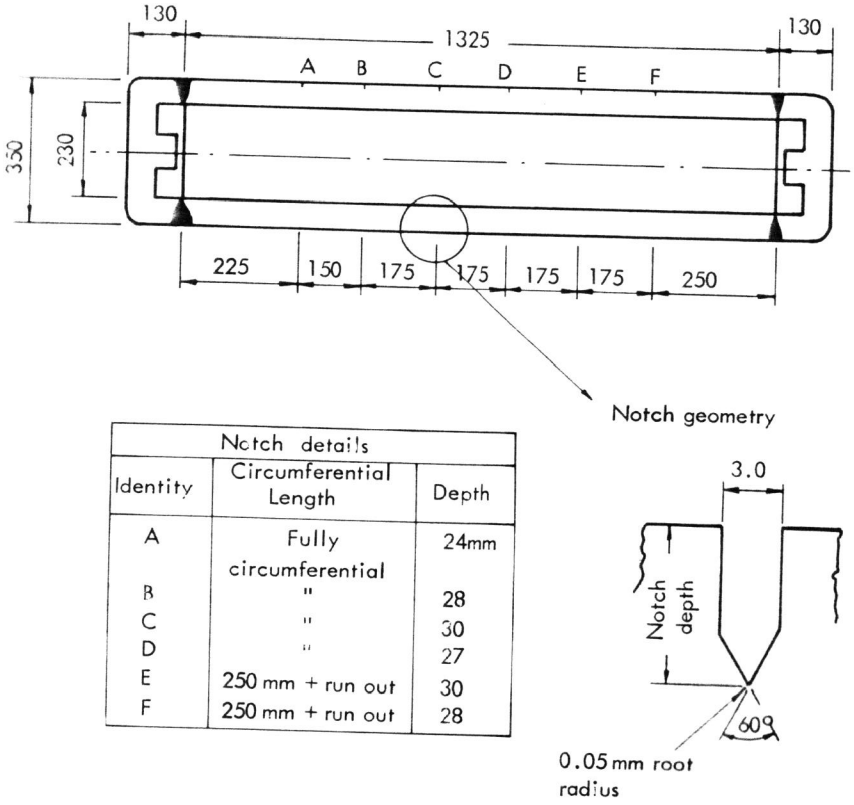

Notch details		
Identity	Circumferential Length	Depth
A	Fully circumferential	24mm
B	"	28
C	"	30
D	"	27
E	250 mm + run out	30
F	250 mm + run out	28

Figure 1 Details of the circumferentially notched pressure vessel.

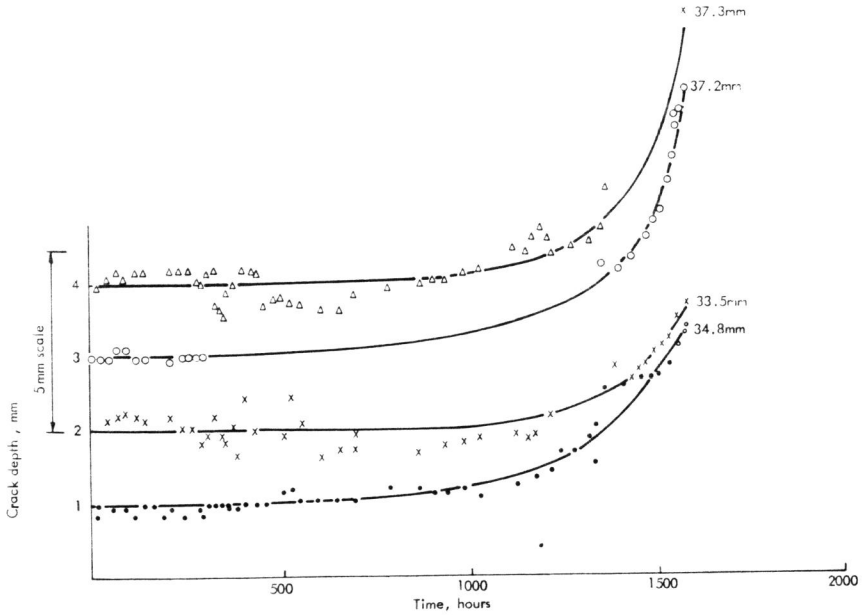

Figure 2 Crack growth measured using the potential drop technique, against time at 838K and 62.5 MPa. The four plots relate to equi-spaced positions around the circumference of the 30mm original notch.

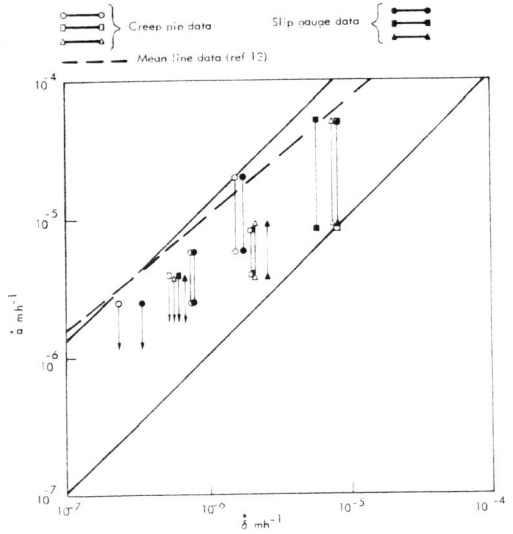

Figure 3 The relationship between creep crack growth rate, $\dot{a}$ and displacement rate, $\dot{\delta}$.

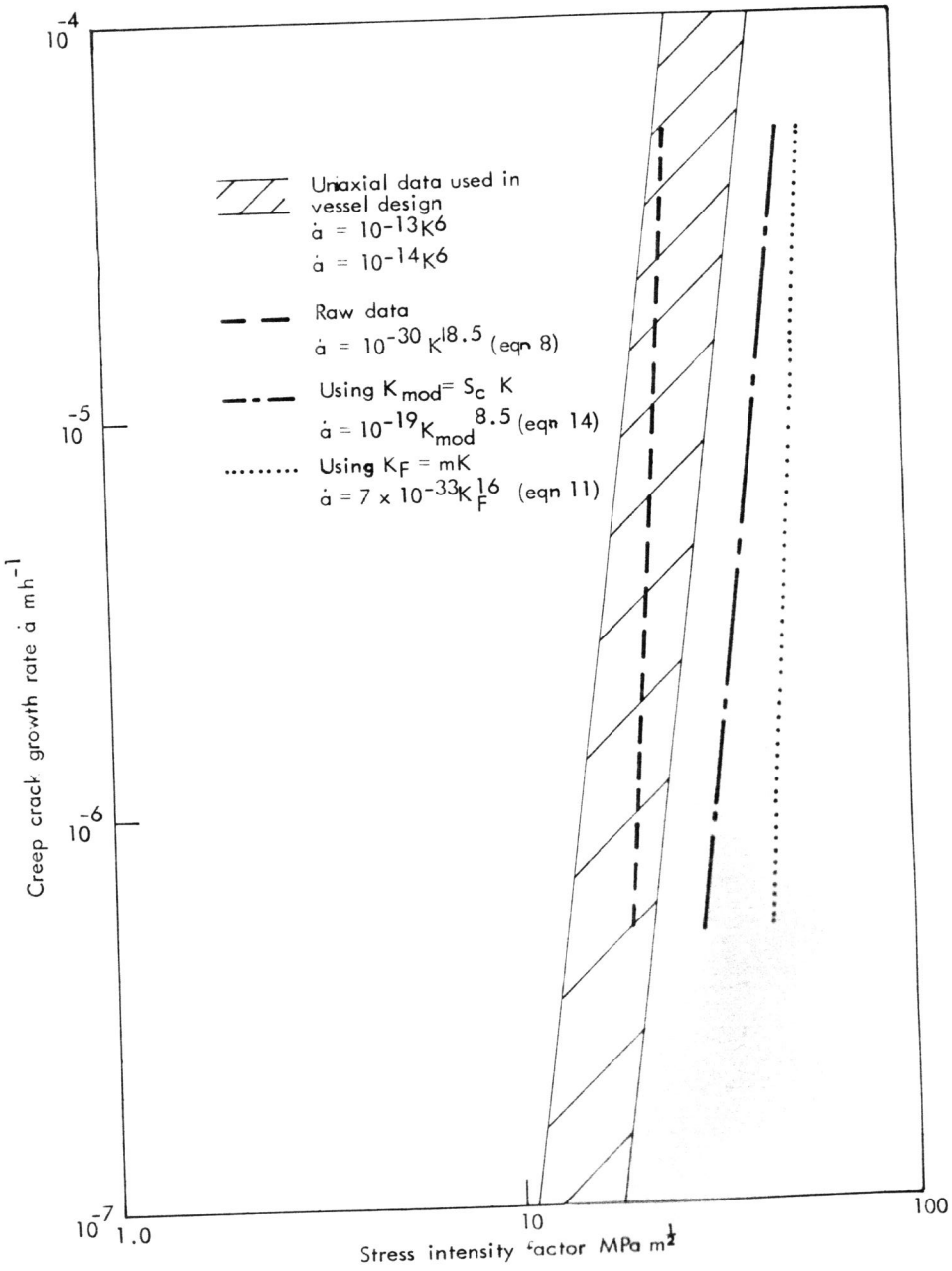

Figure 4 The relationships between creep crack growth rate and stress intensity factor derived from pressure vessel and laboratory data.

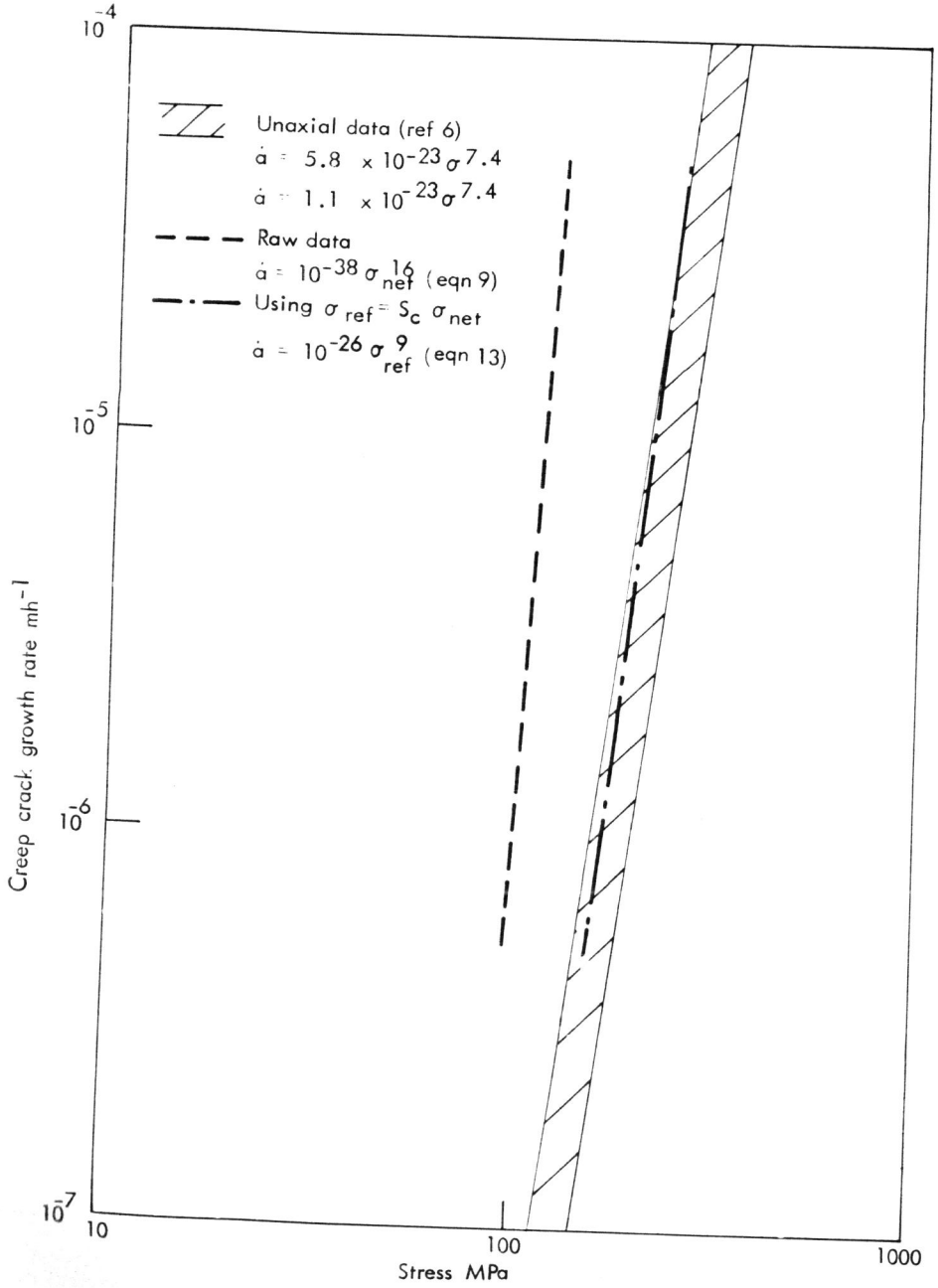

Figure 5 The relationships between creep crack growth rate and reference stress from pressure vessel and laboratory data.